



Topological states in a microscopic model of interacting fermions

Nicolai Lang* and Hans Peter Büchler

Institute for Theoretical Physics III, University of Stuttgart, 70550 Stuttgart, Germany

(Received 16 April 2015; published 29 July 2015)

We present a microscopic model of interacting fermions where the ground state degeneracy is topologically protected. The model is based on a double-wire setup with local interactions in a particle number conserving setting. A compelling property of this model is the exact solvability for its ground states and low energy excitations. We demonstrate the appearance of topologically protected edge states and derive their braiding properties on a microscopic level. We find the non-Abelian statistics of Ising anyons, which can be interpreted as Majorana-like edge states.

DOI: [10.1103/PhysRevB.92.041118](https://doi.org/10.1103/PhysRevB.92.041118)

PACS number(s): 71.10.Pm, 03.67.Lx, 03.75.Ss, 74.25.-q

Introduction. Topologically protected ground state degeneracies in many-body quantum systems, and the closely related (non-Abelian) anyonic statistics, are of special interest from a theoretical point of view [1,2], and have been recognized as promising concepts for scalable fault-tolerant quantum computation [3,4]. A well understood class is topological states with Majorana zero-energy edge modes appearing within mean-field descriptions of topological superconductors [5]. These free fermion theories have been classified exhaustively [6,7], and the properties of the Majorana zero modes at boundaries [8] and in vortices [9] have been characterized. In contrast, interacting and gapless phases are less well understood [10–13], and to which extent existence and non-Abelian properties of edge states carry over to interacting theories is an interesting question lacking conclusive answers [14].

The understanding of topological states is driven by exactly solvable microscopic models; the paradigmatic one for the existence of topologically protected Majorana edge modes is the one-dimensional Majorana chain [8]. It has inspired a variety of proposals for its experimental realization in condensed matter systems [5,15–17], and signatures consistent with Majorana modes have been experimentally observed [18–21]. Nevertheless, these models require large reservoirs to justify their mean-field description, whereas very little is known about the fate of Majorana zero-energy edge modes in intrinsically interacting and particle conserving settings. Previous attempts for number-conserving theories featuring Majorana-like edge states relied either on bosonization [22–26] or on numerical methods [density-matrix renormalization group (DMRG)] [27], while the only exactly solvable models require unphysical long-range interactions [28].

In this Rapid Communication, we present a microscopic, number-conserving theory with *local* interactions that features non-Abelian edge states at the boundaries. The theory allows for an exact derivation of its many-body ground state as well as its low-energy excitations, and thereby provides a viable playground for analyzing its characteristic properties. We find that the ground state is characterized by a condensate of *p*-wave pairs with a topological degeneracy. The Green's function exhibits a revival at the edges, indicating the appearance of edge states. Remarkably, the system can

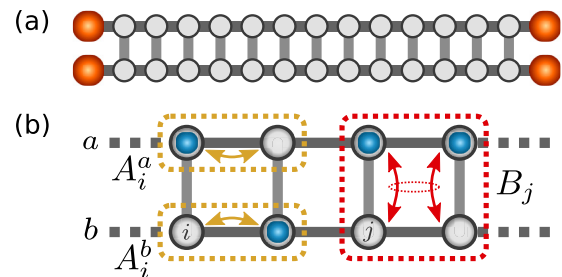


FIG. 1. (Color online) Setup. (a) We consider a double chain (two-leg ladder) of spinless fermions with upper (lower) chain denoted as *a* (*b*). (b) The number-conserving Hamiltonian is given by intrachain terms A_i^x ($x = a, b$) and interchain couplings B_j .

be extended to arbitrary wire networks, which allows us to derive the non-Abelian braiding statistics of the edge states on a microscopic level.

We consider a double chain (two-leg ladder) of spinless fermions with L lattice sites. The fermionic creation operators at site i are described by a_i^\dagger (upper chain) and b_i^\dagger (lower chain) (see Fig. 1). The many-body Hamiltonian $H = H^a + H^b + H^{ab}$ describing the interacting fermion theory combines intrachain contributions H^x ($x = a, b$) as well as interactions H^{ab} between the two chains. The intrachain Hamiltonian takes the form

$$H^x = \sum_{i=1}^{L-1} A_i^x (\mathbb{1} + A_i^x) \quad (1)$$

with the single-particle hopping terms

$$A_i^a = a_i a_{i+1}^\dagger + a_{i+1} a_i^\dagger, \quad A_i^b = b_i b_{i+1}^\dagger + b_{i+1} b_i^\dagger. \quad (2)$$

Consequently, it combines single-particle hopping with a nearest-neighbor attraction $n_i^x + n_{i+1}^x - 2n_i^x n_{i+1}^x$. The interchain interaction H^{ab} takes a similar form

$$H^{ab} = \sum_{i=1}^{L-1} B_i (\mathbb{1} + B_i) \quad (3)$$

with the pair hopping between the two chains

$$B_i = a_i^\dagger a_{i+1}^\dagger b_i b_{i+1} + b_i^\dagger b_{i+1}^\dagger a_i a_{i+1}. \quad (4)$$

It is important to stress that the Hamiltonian H conserves the total number of particles N , which defines the only free

*nicolai@itp3.uni-stuttgart.de

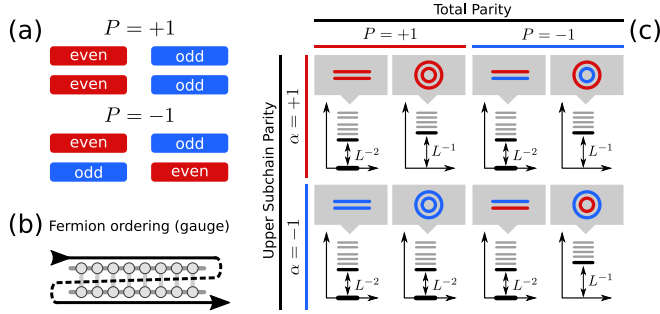


FIG. 2. (Color online) Ground states. (a) For every filling N with parity $P = (-1)^N$, there are two degenerate zero-energy ground states for open boundary conditions, characterized by their (upper) subchain parity $\alpha = P_a$. (b) The chosen fermion gauge leads to the simple description of the ground states given in the text. (c) Behavior of the spectrum in the low-energy sector of symmetry subspaces classified by the total parity P and the subchain parity α . Both open (OBC) and periodic (PBC) boundary conditions are shown; zero-energy states are drawn bold.

parameter of the theory and is conveniently expressed as the filling $\rho = N/2L$. H features two additional, relevant symmetries, namely, (i) the subchain parity $P_x \equiv (-1)^{\sum_i x_i^\dagger x_i}$ ($x = a, b$), and (ii) time-reversal symmetry $\mathcal{T} \equiv K$ represented by complex conjugation K and $\mathcal{T} x_i^{(\dagger)} \mathcal{T}^{-1} \equiv x_i^{(\dagger)}$.

Ground states. In order to derive the ground states analytically, the observation that Hamiltonian H is the sum of local projectors and therefore a locally positive operator is crucial. Then we exploit the fact that any zero-energy ground state must be annihilated by all local terms in (1) and (3) simultaneously. That is, if we find a state with zero energy which is annihilated by all local terms, we can be sure that it is a ground state. This yields a viable method to construct them from scratch—provided zero-energy ground states exist.

For an *open* ladder, there are exactly two degenerate zero-energy ground states for each filling $0 < N < 2L$ [Fig. 2(a)], denoted as $|N, \alpha\rangle$ and characterized by the upper chain parity $\alpha \equiv P_a \in \{+1, -1\}$ (see the Supplemental Material for a rigorous proof [29]). For an appropriate fermion gauge [see Fig. 2(b)], each ground state is given by the equal-weight superposition of distributing N particles on the two chains constrained by the fixed subchain parity α . To cast this in a formal description, we first introduce the fermion number states $|\mathbf{n}\rangle_x$ with $x = a, b$ and $\mathbf{n} \in \{0, 1\}^L$, i.e., $|\mathbf{n}\rangle_a = (a_1^\dagger)^{n_1} \dots (a_i^\dagger)^{n_i} \dots (a_L^\dagger)^{n_L} |0\rangle_a$ for the upper chain with the number of fermions $|\mathbf{n}| = \sum_{i=1}^L n_i$. Then the equal-weight superposition states on each chain with a fixed number of particles reduce to $|n\rangle_x \equiv \sum_{|\mathbf{n}|=n} |\mathbf{n}\rangle_x$; note that this state is not normalized. Finally, the equal-weight superposition with fixed particle number N and subchain parity α can be written as

$$|N, \alpha\rangle = \mathcal{N}_{L, N, \alpha}^{-1/2} \sum_{n, (-1)^n = \alpha} |\mathbf{n}\rangle_a |N - n\rangle_b, \quad (5)$$

where $\mathcal{N}_{L, N, \alpha}^{-1/2}$ is the normalization factor that counts the number of superimposed fermion configurations.

In contrast, for a *closed* ladder the situation is more subtle: For *even* total particle number $N = 2K$, there is a unique zero-energy ground state $|2K, -1\rangle$ in the odd-odd ($\alpha = -1$)

subchain-parity sector, whereas in the odd- N sectors all states are lifted to finite energy. This is summarized in Fig. 2(c) where the low-energy scaling is given as well (see below).

At this point it seems advisable to compare these ground states with those of a *single* Majorana chain (Kitaev's chain), which in analogy features two zero-energy ground states for open boundary conditions [8]: For vanishing chemical potential (perfectly localized edge modes), the ground states of the Majorana chain are given by the equal-weight superposition of particle number states with fixed (global) parity. In contrast, here the chains act as mutual particle reservoirs and the ground state degeneracy arises due to two admissible subchain-parity configurations within each fixed particle number sector.

We start exploiting the concise description of the ground states, and derive simple expressions for density correlations, superfluid order parameter, and the Green's function (single-particle correlation). To this end, it proves useful to define the *parity-split binomial coefficients* (PsBCs) which count the configurations to distribute N particles among $\sum_{i=1}^g L_i$ sites with the additional constraint that the parity of subsystem L_i ($1 \leq i < g$) is fixed by $\alpha_i = \pm 1$,

$$\binom{L_1, \dots, L_g}{\alpha_1, \dots, \alpha_{g-1}}_N \equiv \sum_{n_1, \dots, n_{g-1}} \binom{L_g}{N - \sum_{i=1}^{g-1} n_i} \prod_{i=1}^{g-1} \binom{L_i}{n_i} \delta_{n_i}^{\alpha_i} \quad (6)$$

with $\delta_{n_i}^{\alpha_i} \equiv [1 + \alpha_i (-1)^{n_i}]/2$. Although we are not aware of simple analytical expressions (except for special cases; see Supplemental Material), the PsBCs can easily be evaluated numerically. Due to the simple structure of the ground states, all correlation functions and expectation values of $|N, \alpha\rangle$ can be rewritten in terms of finite combinations of PsBCs. E.g., the normalization of the two ground states reads $\mathcal{N}_{L, N, \alpha} = \binom{L, L}{\alpha}_N$.

We find that the density-density correlation function factorizes, $\langle x_i^\dagger x_i y_j^\dagger y_j \rangle \rightarrow \rho^2$ for $i \neq j$; $x, y \in \{a, b\}$ in the thermodynamic limit $L, N \rightarrow \infty$ with fixed particle density ρ . The pair correlations read $|\langle x_i^\dagger x_{i+1}^\dagger y_j y_{j+1} \rangle| \rightarrow \rho^2 (1 - \rho)^2$ for $i \neq j$; $x, y \in \{a, b\}$, and indicate a condensate of p -wave pairs with true long-range order. Note that the results for both correlators do *not* depend on the subchain parity α of the ground states. This is true up to exponential corrections vanishing with $L \rightarrow \infty$. For particularly symmetric setups (e.g., $x \neq y$ and N odd) these corrections even vanish identically.

The intrachain Green's function (indicating single-particle off-diagonal long-range order [30]) can be expressed in terms of PsBCs ($j > i + 1$)

$$\langle a_i^\dagger a_j \rangle = \mathcal{N}_{L, N, \alpha}^{-1} [\Lambda_{+1, -\alpha} - \Lambda_{-1, \alpha}], \quad (7)$$

where $\Lambda_{\alpha_1, \alpha_2} \equiv \binom{j-i-1, L-j+i-1, L}{\alpha_1, \alpha_2}_{N-1}$. See the Supplemental Material for a detailed derivation. In the thermodynamic limit one finds exponentially decaying correlations in the bulk [see Fig. 3(a)],

$$\langle x_i^\dagger x_j \rangle = e^{-\gamma(\rho)|i-j|} \quad \text{for } 1 \ll i, j \ll L; x \in \{a, b\}, \quad (8)$$

where γ is some function of the filling with $0 < \gamma(\rho) \leq \infty$ and $\gamma(1/2) = \infty$. The boundary terms read $|\langle a_1^\dagger a_L \rangle| \rightarrow \rho(1 - \rho)$

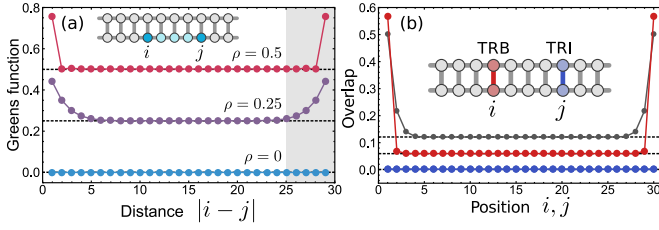


FIG. 3. (Color online) Ground state properties. (a) Intrachain single-particle correlation $\langle a_i^\dagger a_j \rangle$ (Green's function) as a function of the distance $|i - j|$ for various fillings ρ and a chain of length $L = 30$. The revival for $|i - j| \sim L$ indicates exponentially localized edge states (gray region). (b) Overlap of the ground states for time-reversal invariant (TRI) and breaking (TRB) perturbations of H in dependence on the position i, j of the subchain-parity violating single-particle hopping (blue: $\rho = 0.5$ TRI; red: $\rho = 0.5$ TRB; gray: $\rho = 0.25$ TRB).

in the thermodynamic limit, indicating the existence of exponentially localized edge states [Fig. 3(a)].

The *topological protection* of the ground state degeneracy is most conveniently characterized in terms of their indistinguishability by any local perturbation [14,31]. Let \mathcal{O} be an arbitrary local (Hermitian) operator. Then the expectation values $\langle \alpha | \mathcal{O} | \alpha \rangle$ and $\langle -\alpha | \mathcal{O} | -\alpha \rangle$ are identical up to an exponentially small correction—as follows from the above analysis of the correlation functions. However, for operators violating the subchain parity P_x , also the overlap $\langle -\alpha | \mathcal{O} | \alpha \rangle$ must be taken into account. Then the situation is more subtle. We illustrate this for the simplest case of a single-particle interchain hopping (the statements can be generalized to more complex P_x -violating terms, though). Let $\mathcal{O}_j = e^{i\phi} a_j^\dagger b_j + e^{-i\phi} b_j^\dagger a_j$ with complex hopping phase $\phi \in [0, 2\pi)$. Splitting this perturbation into time-reversal invariant (TRI) and breaking (TRB) contributions, one finds by evaluating the corresponding PsBCs,

$$\text{TRI} : \langle -\alpha | a_\delta^\dagger b_\delta + b_\delta^\dagger a_\delta | \alpha \rangle \rightarrow 0, \quad (9a)$$

$$\text{TRB} : \langle -\alpha | i a_\delta^\dagger b_\delta - i b_\delta^\dagger a_\delta | \alpha \rangle \rightarrow e^{-\mu(\rho)\delta} \quad (9b)$$

for the distance δ from the edges of the ladder, $\delta \ll L$ when $L \rightarrow \infty$ and ρ is fixed. These site-dependent overlaps are illustrated in Fig. 3(b). Thus the topological ground state degeneracy for the double-wire setup can either be protected by time-reversal symmetry \mathcal{T} or subchain parity P_x , and is only spoiled if both symmetries are broken at the same time. The latter, however, is not surprising as the two edge states on the upper and lower wires are not spatially separated. We will show below that our model can be generalized to wire networks, where the different edge states become spatially separated. Then it follows immediately that the topological properties are protected against *any* local operator \mathcal{O} conserving the total number of particles.

Ground state entanglement. Another well-known signature of topological states is a stable degeneracy of the entanglement spectrum (ES) [32–34]. In our case, the ES of the ground states $|N, \alpha\rangle$ with respect to a bipartition ($\mathbb{S} | \mathbb{L} \setminus \mathbb{S}$) of the ladder [see

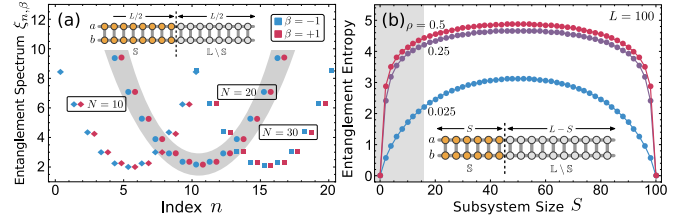


FIG. 4. (Color online) Entanglement. (a) Two branches ($\beta = \pm 1$: red/blue) of the entanglement spectrum for a chain of length $L = 20$ and splitting $S = 10$ with fillings $N = 10, 20, 30$ (diamonds, circles, squares, respectively). The half-filling branch is highlighted gray. Physically, the index n describes the subsystem filling while β describes the subsystem subchain parity. This illustrates the twofold degeneracy of the entanglement spectrum. (b) The entanglement entropy S^{ent} as a function of subsystem size S for various fillings ρ . It obeys an area law with logarithmic corrections.

inset of Fig. 4(b)] is given by the Schmidt decomposition

$$|N, \alpha\rangle = \sum_n \sum_{\beta=\pm 1} e^{-\xi_{n,\beta}/2} |n, \beta\rangle_{\mathbb{S}} |N - n, \alpha\beta\rangle_{\mathbb{L} \setminus \mathbb{S}} \quad (10)$$

and can be written in terms of PsBCs,

$$\xi_{n,\beta} = -\ln \left[\binom{L-S, L-S}{\alpha\beta}_{N-n} \binom{S, S}{\beta}_n / \binom{L, L}{\alpha}_N \right], \quad (11)$$

where $\max\{0, N - 2L + 2S\} \leq n \leq \min\{N, 2S\}$ and $\beta = \pm 1$. The $\beta = \pm 1$ branches of the spectra for a half-split system of length $L = 20$ are shown in Fig. 4(a) for different fillings N and reveal the twofold degeneracy of the ES due to the subsystem subchain parity β .

In addition, the scaling of the entanglement of a subsystem \mathbb{S} with the environmental system as a function of the subsystem size S in terms of the entanglement entropy $S^{\text{ent}}[\mathbb{S}] \equiv -\text{Tr}[\rho_{\mathbb{S}} \ln \rho_{\mathbb{S}}]$, with reduced density matrix $\rho_{\mathbb{S}} = \text{Tr}_{\mathbb{L} \setminus \mathbb{S}}[\rho]$, yields insight into the low-energy physics of the theory. S^{ent} can easily be computed from the entanglement spectrum via $S^{\text{ent}}[\mathbb{S}] = \sum_{n,\beta} e^{-\xi_{n,\beta}} \xi_{n,\beta}$. Figure 4(b) shows the (filling dependent) variation of entanglement between a growing subsystem and its environmental system as a function of the subsystem size S : It obeys an area law with logarithmic corrections, as expected from a critical (gapless) one-dimensional system. That is, in contrast to the gapped Majorana chain, here we face a low-energy theory of gapless Goldstone modes due to particle number conservation. With this in mind, we have a closer look at the low-energy excitations.

Low-energy excitations. The single-chain Hamiltonians H^x for an open ladder can be mapped to the ferromagnetic, isotropic Heisenberg chain via a Jordan-Wigner transformation. The complete spectrum of H^x is therefore accessible via the Bethe ansatz [35]. Exploiting this mapping, it is possible to construct the analog of single magnon states for our theory. These exact low-energy eigenstates for the open *double* chain take the form

$$|k; N, \alpha\rangle = P_1^a(k) \oplus P_1^b(k) |N, \alpha\rangle \quad (12)$$

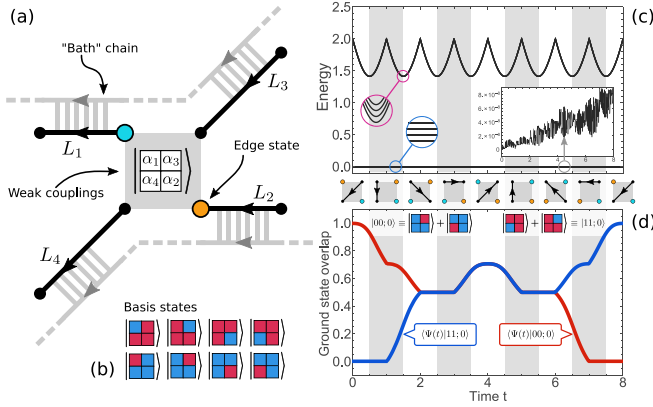


FIG. 5. (Color online) Braiding. (a) Setup of four open chains L_i , $i = 1, 2, 3, 4$ (black) with controllable weak single-particle couplings between the inner four end points. The partner chains (gray) are not involved in the braiding and can be disregarded. (b) The dynamics takes place in the eight-dimensional Hilbert space spanned by the subchain-parity eigenstates with fixed total parity $\alpha = \alpha_1 \alpha_2 \alpha_3 \alpha_4 = -1$. The colors denote the subchain parities α_i of the four black chains. (c) Spectrum of the weak coupling Hamiltonian during the braiding procedure depicted below the plot. A black arrow indicates single-particle hopping. There are four degenerate zero-energy ground states. The deviation from zero energy (perfect adiabaticity) due to the finite time evolution is shown in the inset ($\sim 10^{-8}$). (d) Time evolution for the initial zero-energy state $|00;0\rangle$. Shown are the (moduli of the) overlaps with $|00;0\rangle$ and $|11;0\rangle$ (see inset).

with momentum $k = m\frac{\pi}{L}$, $0 \leq m < L$, and the operator

$$P_1^x(k) = \sum_{j=1}^L \cos\left[\frac{k}{2}(2j-1)\right] (-1)^{x_j^\dagger x_j}. \quad (13)$$

The eigenenergies are given by a quadratic excitation spectrum $E_k = 4 \sin^2 \frac{k}{2}$. This behavior of the Goldstone mode is in excellent agreement with the appearance of a true condensate and vanishing compressibility; recall that for any fixed number of particles there is a zero-energy ground state. An equivalent behavior is well known for noninteracting bosons and the ferromagnetic Heisenberg model in one dimension. The interpretation of these features is that our model is exactly solvable at a critical point.

Wire networks and non-Abelian statistics. A crucial aspect of our model is that the derivation of the exact zero-energy ground states can be straightforwardly generalized to much more complicated wire networks consisting of open and closed single chains sectionally connected to ladder segments with arbitrary positive coupling strengths [see Fig. 5(a) for an example]; the general formalism is presented in the Supplemental Material. It follows immediately that the ground state degeneracy scales as $2^{E/2-1}$ with $E \geq 2$ the number of open subchain ends. This scaling is in agreement with the interpretation of the localized edge states as interacting

equivalent of Majorana zero modes. In order to provide a rigorous proof of the topological properties characterizing the localized edge states, we derive the full braiding statistics. Note that the gap Δ closes algebraically, $\Delta \propto 1/L^2$ [Fig. 2(c)]. This still allows for a generalized notion of braiding and thereby probing the edge state statistics [14].

In order to braid two localized edge states, we consider the wire network of four open subchains coupled by a common “bath” chain depicted in Fig. 5(a) and described by H_0 . Only the highlighted chains L_i ($i = 1, \dots, 4$) take part in the braiding evolution. Thus the grayed out subchain can henceforth be neglected and considered as a “bath,” the effect of which is fully incorporated into the exactly known ground states. Note that the zero-energy states of the uncoupled subchains are given by the total filling N and the subchain parities $\alpha_1, \dots, \alpha_4$, spanning a $2^4 = 16$ dimensional ground state space in each particle number sector. As we are only considering interactions between the four subchains, the total subchain parity $\alpha = \prod_i \alpha_i$ is conserved and may be fixed at $\alpha = -1$, reducing the number of relevant ground states to eight [see Fig. 5(b)]. The braiding of the edge states is described by $H_{\text{int}}(t)$ and achieved by adiabatically turning off the coupling between two edges and turning on the coupling between the next two edges; the full sequence of couplings for the winding of two edge states around each other is shown below Fig. 5(c), where arrows indicate single-particle couplings analogous to $A_i(\mathbb{1} + A_i)$.

The analysis is performed by the full numerical time evolution of the Hamiltonian $H(t) = H_0 + \varepsilon/L^2 H_{\text{int}}(t)$ with $\varepsilon \ll 1$ and $0 \leq t \leq 8$ to guarantee the (quasi)-adiabatic evolution. Starting with the initial zero-energy state $|00;0\rangle$ [Fig. 5(d)] characterized by $\alpha_1 = -1 = \alpha_2$ and $\alpha_3 \alpha_4 = -1$, yields the orthogonal final state $|11;0\rangle = \exp[-i \int dt H_{\text{int}}(t)] |00;0\rangle$, characterized by $\alpha_1 = +1 = \alpha_2$ and $\alpha_3 \alpha_4 = -1$. Repeating the analysis for alternative braiding operations, we find the non-Abelian holonomy acting on the degenerate ground state space that qualifies the edge states as Ising anyons [36], which corresponds to the braiding statistics of Majorana edge modes in noninteracting theories.

Conclusion. We presented a microscopic model of interacting fermions giving rise to a gapless topological state with non-Abelian edge states. The system is at a critical point and certain perturbations to the Hamiltonian will drive the system into a phase separated state (e.g., increasing the attractive interactions), while we expect resilience of the topological properties against other perturbations (e.g., increasing the hopping). Then the ground state should be well described by an approach based on bosonization similar to [22–26], and might be connected to the state studied with DMRG [27].

Note added. Recently, we became aware of related results studied by Iemini *et al.* [37].

Acknowledgments. H.P.B thanks E. Altman for his hospitality at the Weizmann Institute. We acknowledge support by the Deutsche Forschungsgemeinschaft (DFG) within SFB/TRR 21.

[1] D. Arovas, J. R. Schrieffer, and F. Wilczek, *Phys. Rev. Lett.* **53**, 722 (1984).

[2] M. Levin and X.-G. Wen, *Phys. Rev. B* **67**, 245316 (2003).

[3] A. Kitaev, *Ann. Phys.* **303**, 2 (2003).

- [4] C. Nayak, S. H. Simon, A. Stern, M. Freedman, and S. Das Sarma, *Rev. Mod. Phys.* **80**, 1083 (2008).
- [5] C. W. J. Beenakker, [arXiv:1407.2131](https://arxiv.org/abs/1407.2131) [Rev. Mod. Phys. (to be published)].
- [6] A. Kitaev, *Advances in Theoretical Physics: Landau Memorial Conference*, AIP Conf. Proc. No. 1134 (AIP, Melville, NY, 2009), p. 22.
- [7] S. Ryu, A. P. Schnyder, A. Furusaki, and A. W. W. Ludwig, *New J. Phys.* **12**, 065010 (2010).
- [8] A. Y. Kitaev, *Phys.-Usp.* **44**, 131 (2001).
- [9] D. A. Ivanov, *Phys. Rev. Lett.* **86**, 268 (2001).
- [10] L. Fidkowski and A. Kitaev, *Phys. Rev. B* **83**, 075103 (2011).
- [11] N. Schuch, D. Pérez-García, and I. Cirac, *Phys. Rev. B* **84**, 165139 (2011).
- [12] X. Chen, Z.-C. Gu, and X.-G. Wen, *Phys. Rev. B* **83**, 035107 (2011).
- [13] X.-G. Wen, *Phys. Rev. B* **89**, 035147 (2014).
- [14] P. Bonderson and C. Nayak, *Phys. Rev. B* **87**, 195451 (2013).
- [15] R. M. Lutchyn, J. D. Sau, and S. Das Sarma, *Phys. Rev. Lett.* **105**, 077001 (2010).
- [16] Y. Oreg, G. Refael, and F. von Oppen, *Phys. Rev. Lett.* **105**, 177002 (2010).
- [17] J. Alicea, *Rep. Prog. Phys.* **75**, 076501 (2012).
- [18] V. Mourik, K. Zuo, S. M. Frolov, S. R. Plissard, E. P. A. M. Bakkers, and L. P. Kouwenhoven, *Science* **336**, 1003 (2012).
- [19] A. Das, Y. Ronen, Y. Most, Y. Oreg, M. Heiblum, and H. Shtrikman, *Nat. Phys.* **8**, 887 (2012).
- [20] S. Nadj-Perge, I. K. Drozdov, J. Li, H. Chen, S. Jeon, J. Seo, A. H. MacDonald, B. A. Bernevig, and A. Yazdani, *Science* **346**, 602 (2014).
- [21] J.-P. Xu, M.-X. Wang, Z. L. Liu, J.-F. Ge, X. Yang, C. Liu, Z. A. Xu, D. Guan, C. L. Gao, D. Qian, Y. Liu, Q.-H. Wang, F.-C. Zhang, Q.-K. Xue, and J.-F. Jia, *Phys. Rev. Lett.* **114**, 017001 (2015).
- [22] M. Cheng and H.-H. Tu, *Phys. Rev. B* **84**, 094503 (2011).
- [23] L. Fidkowski, R. M. Lutchyn, C. Nayak, and M. P. A. Fisher, *Phys. Rev. B* **84**, 195436 (2011).
- [24] J. D. Sau, B. I. Halperin, K. Flensberg, and S. Das Sarma, *Phys. Rev. B* **84**, 144509 (2011).
- [25] J. Ruhman, E. Berg, and E. Altman, *Phys. Rev. Lett.* **114**, 100401 (2015).
- [26] A. Keselman and E. Berg, *Phys. Rev. B* **91**, 235309 (2015).
- [27] C. V. Kraus, M. Dalmonte, M. A. Baranov, A. M. Läuchli, and P. Zoller, *Phys. Rev. Lett.* **111**, 173004 (2013).
- [28] G. Ortiz, J. Dukelsky, E. Cobanera, C. Eсеbbag, and C. Beenakker, *Phys. Rev. Lett.* **113**, 267002 (2014).
- [29] See Supplemental Material at <http://link.aps.org/supplemental/10.1103/PhysRevB.92.041118> for a rigorous derivation of the ground states, their expectation values and correlators, analytical and numerical properties of the spectral gap, an extension of the braiding scheme to wire networks, and a detailed discussion of the braiding results.
- [30] C. N. Yang, *Rev. Mod. Phys.* **34**, 694 (1962).
- [31] Z. Nussinov and G. Ortiz, *Ann. Phys.* **324**, 977 (2009).
- [32] H. Li and F. D. M. Haldane, *Phys. Rev. Lett.* **101**, 010504 (2008).
- [33] F. Pollmann, A. M. Turner, E. Berg, and M. Oshikawa, *Phys. Rev. B* **81**, 064439 (2010).
- [34] A. M. Turner, F. Pollmann, and E. Berg, *Phys. Rev. B* **83**, 075102 (2011).
- [35] H. Bethe, *Z. Phys.* **71**, 205 (1931).
- [36] A. Kitaev, *Ann. Phys.* **321**, 2 (2006).
- [37] F. Iemini, L. Mazza, D. Rossini, S. Diehl, and R. Fazio, [arXiv:1504.04230](https://arxiv.org/abs/1504.04230) [Phys. Rev. Lett. (to be published)].